ISBN: 978-3-95450-236-3 ISSN: 2673-7027 doi:10.18429/JACoW-eeFACT2022-WEZAT0202

LESSONS LEARNED FROM OPERATIONAL EXPERIENCE OF SuperKEKB IR MAGNETS AND UPGRADE PLANS FOR THE FUTURE

Y. Arimoto*, K. Aoki, M. Kawai, T. Kawamoto, M. Maszawa, S. Nakamura, Y. Ohsawa, N. Ohuichi, T. Oki, R. Ueki, X. Wang, H. Yamaoka, Z. Zong, KEK, Tsukuba, Japan

Abstract

SuperKEKB is an upgraded accelerator from KEKB, aiming at a luminosity of $6 \times 10^{35}\,\mathrm{cm^{-2}\,s^{-1}}$. It is currently in operation, setting new luminosity records. We have completely redesigned the final-focus-magnet system to achieve the target luminosity by upgrading from KEKB to SuperKEKB. After the completion of the system, it started its practical operation in 2018 after measuring the magnetic field in IR. The operation is generally stable, but some troubles have occurred. One of them is a quench. Radiation related to stored beam deposit energy on the superconducting coil. And then, we experienced the tune variations in LER, which suggested fluctuations in the main quadrupole magnetic field, and measurements using the R & D magnet demonstrated this phenomenon. In addition, we are seeking a plan to upgrade the QCS for the long shutdown around 2027.

INTRODUCTION

KEKB is a B-Factory and is an e^+/e^- collider operated from 1998 to 2010 [1]. It achieved a peak luminosity of $2.11 \times 10^{34}\,\mathrm{cm^{-2}\,s^{-1}}$ and an integrated luminosity of $1040\,\mathrm{fb^{-1}}$. The Belle experiment using KEKB has achieved many physics results. To make precise measurements of weak interaction parameters and find new physics beyond the Standard Model, the KEKB has been upgraded to the SuperKEKB [2]. It aims at a peak luminosity of $6 \times 10^{35}\,\mathrm{cm^{-2}\,s^{-1}}$ and the integrated luminosity of $50\,\mathrm{ab^{-1}}$. The operation of the SuperKEKB started from 2018 and achieved the peak luminosity of $4.7 \times 10^{34}\,\mathrm{cm^{-2}\,s^{-1}}$ up to 2022 [3].

FINAL FOCUS SYSTEM OF KEKB AND SUPERKEKB

One of the critical components for the accelerator upgrade from KEKB to SuperKEKB is a final focus system with superconducting (SC) magnets called QCS. At an interaction point (IP), a design vertical-beam size, σ_y^* of SuperKEKB is 50 nm and is 20 times smaller than KEKB.

To achieve this, the QCS system designed for SuperKEKB has independent quadrupole doublets for each ring. For the KEKB-QCS (in this section, we denote this as K-QCS), the electron and positron beam went through the same quadrupole magnets of the QCS. So, the SuperKEKB-QCS (in this section, we denote this as SK-QCS) consists of eight quadrupole doublets; on the other hand, the K-QCS has two quadrupole magnets [4, 5]. Figures 1 and 2 show schematic layouts of the QCS of KEKB and SuperKEKB, respectively. The SK-QCS also has the leak field cancel magnets; they cancel the leak field from QC1LP and QC1RP to HER. The four solenoids of the SK-QCS compensate for the integral solenoid field of Belle II detector , while the K-QCS has two compensation solenoids.

Table 1: KEKB and SuperKEKB Main Parameters

	KEKB		SuperKEKB	
	LER	HER	LER	HER
E [GeV]	3.5	8.0	4.0	7.0
θ_{cross} [mrad]	22		83	
β_y^* [mm]	5.9	5.9	0.27	0.30
σ_y^* [nm]	900	900	48	62

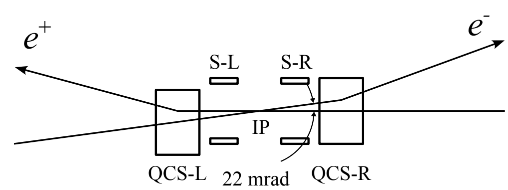

Figure 1: The schematic layout of the KEKB-QCS. S-L and S-R are the compensation solenoids, and the QCS-L and QCS-R are the SC quarupole magnets.

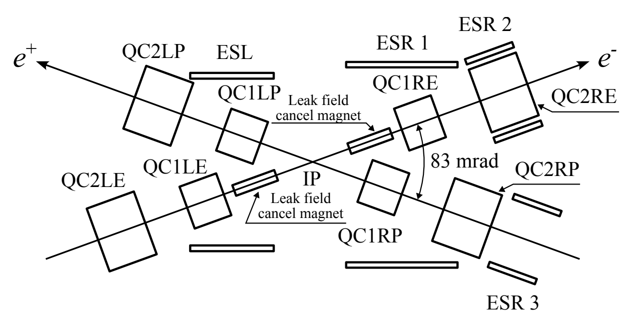

Figure 2: Schematic layout of SuperKEKB-QCS. The magnets representing with "QC" at beginning are the superconducting quadrupole magnets. The leak field cancel magnets are canceling the leak field from QC1RP and QC1LP quads. ESL, ESR1, ESR2, and ESR3 are the compensation solenoids.

Tables 2 and 3 show the main parameters for the quadrupole magnets of KEK and SuperKEKB, respectively. The letter "L" or "R" in all magnet names indicates the magnet on the left or right side of the IP, viewing the IP from the center of the accelerator ring, respectively. The QCS-L and QCS-R magnets are the vertical-focusing quadrupole magnets for KEKB in Table 2. The vertical-focusing quadrupole

* yasushi.arimoto@kek.jp

ISBN: 978-3-95450-236-3 ISSN: 2673-7027 doi:10.18429/JACoW-eeFACT2022-WEZAT0202

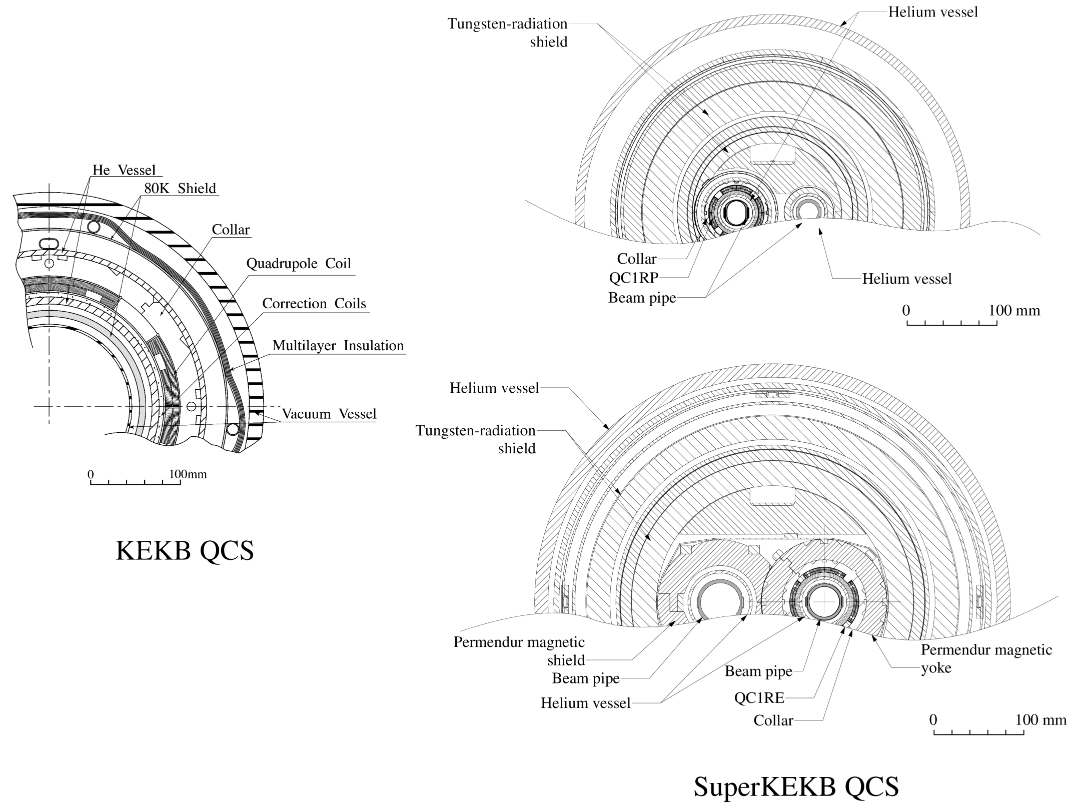

Figure 3: The cross sections of KEKB-QCS [4] and QC1RP and QC1RE for SuperKEKB QCS.

magnets of SuperKEKB are the QC1LP(RP) magnet and the QC1LE(RE) magnet. The QC1LP(RP) and QC1LE(RE) magnets have a B-field gradient of around 70 T/m, and they are three times larger than the QCS-L(R) magnet. Figure 3 shows the cross sections of K-QCS and SK-QCS. The aperture of the QC1LP(RP) and QC1LE(RE) magnets are ten times smaller than QCS-L(-R) magnet.

The SK-QCS has two-refrigerator units whose power is 250 kW at 4.4 K for one unit. We repurposed these refrigerators from TRISTAN and KEKB [6]. The K-QCS has one refrigerator unit repurposed from TRISTAN [4].

The SK-QCS is a more complex system with more SC magnets than K-QCS. Figure 4 shows the entire layout of the SK-QCS magnet and the Belle II solenoid magnet.

Table 2: The main parameters of the QCS quadrupole magnets for KEKB [4]. Here, G is a B-field gradient, I is an operation current. r_{in} is the inner radius of the SC conductor, and L_{eff} is the effective length of the quadrupole field.

Magnet Name	G [T/m]	I [A]	r_{in} [mm]	L_{eff} [mm]
QCS-L	21.66	2963	260	483
QCS-R	21.73	2963	260	385

Table 3: The main parameters of the QCS quadrupole magnets for SuperKEKB. Here, G is a B-field gradient at the operation current, I on April 11th, 2020 [6].

Magnet Name	G	I	r_{in}	L_{eff}
QC1LP	67.8	1598	25.0	334
QC1RP	67.8	1599	25.0	334
QC2LP	28.1	879	53.8	410
QC2RP	28.2	882	53.8	410
QC1LE	72.4	1581	33.0	373
QC1RE	68.6	1499	33.0	373
QC2LE	29.1	1001	59.3	537
QC2RE	30.8	1249	59.3	419

MAGNETIC MEASUREMENTS

We performed several magnetic measurements at the interaction region (IR). The solenoid field generates the electromagnetic force of 52.5 kN and 33.7 kN on the ESL and ESR1, respectively; as a result, the magnets would move [6]. Moreover, the magnet yoke would exhibit magnetic saturation. Since it is not easy to calculate these effects precisely, we performed the in-sites measurement despite taking time and effort.

We had three types of magnetic measurements, a measurement of B-field multipole with harmonic coils, a measurement of the magnet centers with a single stretched wire

ISBN: 978-3-95450-236-3 ISSN: 2673-7027 doi:10.18429/JACoW-eeFACT2022-WEZAT0202

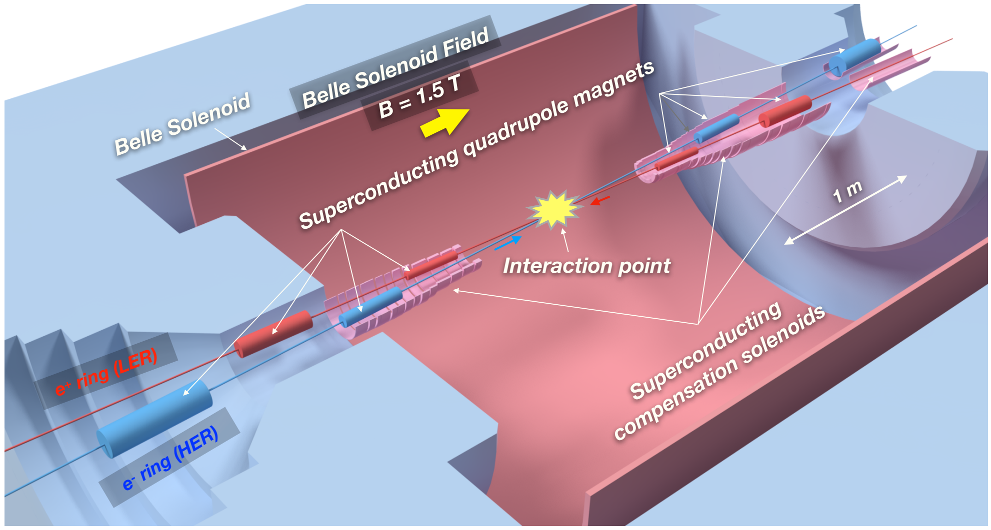

Figure 4: The entire layout of the QCS in the Belle II detector.

(SSW) method, and a measurement of solenoid field with a Hall probe [6].

Measurement of Higher Order Harmonics with Harmonic Coils

The *B*-field of the quadrupole magnet is expanded in multipoles;

$$B(x, y) = 10^{-4} B_2 \sum_{n=1}^{\infty} (b_n + i a_n) \left(\frac{x + iy}{R_{\text{ref}}} \right)^{n-1} \tag{1}$$

here, B_2 is the amplitude of the quadrupole field at the reference radius, R_{ref}, and b_n and a_n are the normal and skew multipoles, respectively. Here, although b_n and a_n are non-dimensional values, we use the "units" as a unit of them. The target higher order multipoles is less than one unit.

Our harmonic coil system has long-winding coils to measure integral *B*-field and short-winding coils to measure axial profiles. We have several kinds of winding radii for each coil. The length of the short coil is 20 mm, and that of long coils is 595-795 mm and longer than the length of the magnets.

The measured integral field with the long coils exhibits slightly larger error fields for allowed components; the other components less than 1-2 units except for the QC2RE quadrupole magnet [6]]. The QC2RE quadrupole magnet exhibit the skew sextupole component of 20 units and 8 units for skew octupole components when the Belle II and the compensation solenoids are turned on. The axial solenoid field has a maximum distance of the IP of 2620 mm. The asymmetric shape of the iron frame causes this.

The QC2RE, ESR2, and ESR3 are contained in an iron structure to shield the solenoid field. The frame is asymmetrical in shape to extract SC wires. Figure 5 shows a perse view of a 3D CAD drawing of the iron structure. The left figure is the iron structure view from the non-IP side. As can be seen from this figure, the shape is asymmetrical at the end. In order to quantitatively investigate the effect of the field quality and to compare it with the measured values, we modeled the iron structure shape on the IP side and calculated it with Opera3D. For simplicity, the model has top-bottom symmetry, and the shape on the non-IP side is a circle. Figure 6 shows an axial profile of the QC2RE quadrupole obtained by energizing all the solenoids. The horizontal axis is the HER beam axis, and the origin is the IP. The measurement and calculation results are solid lines and dashed lines, respectively. Figure 6-(a),-(b), and -(c) are the profiles of skew quadrupole, sextupole, and octupole components at $R_{\text{ref}} = 35$ mm, respectively. At the bottom of these plots, the top view of the QC2RE magnet and the iron structure is illustrated with the same scale and position. At both ends of the iron structure, the plots for all components show a sharp peak error field, and the calculation represents good agreement with the measurement at the IP side. Since the model reproduces the actual geometry only on the IP side, the non-IP side does not reproduce the measurement result.

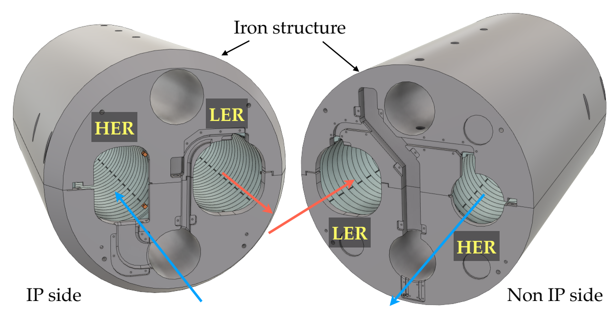

Figure 5: The perse view of the iron structure of the QC2RE. The left is the view from the IP side, and the right is the view from the non-IP side. The QC2RE locates at the HER axis.

Measurement of Magnet Center

We measured the magnet centers of the quadrupole magnets with the single stretched wire (SSW) method [7]. A

ISBN: 978-3-95450-236-3 ISSN: 2673-7027 doi:10.18429/JACoW-eeFACT2022-WEZAT0202

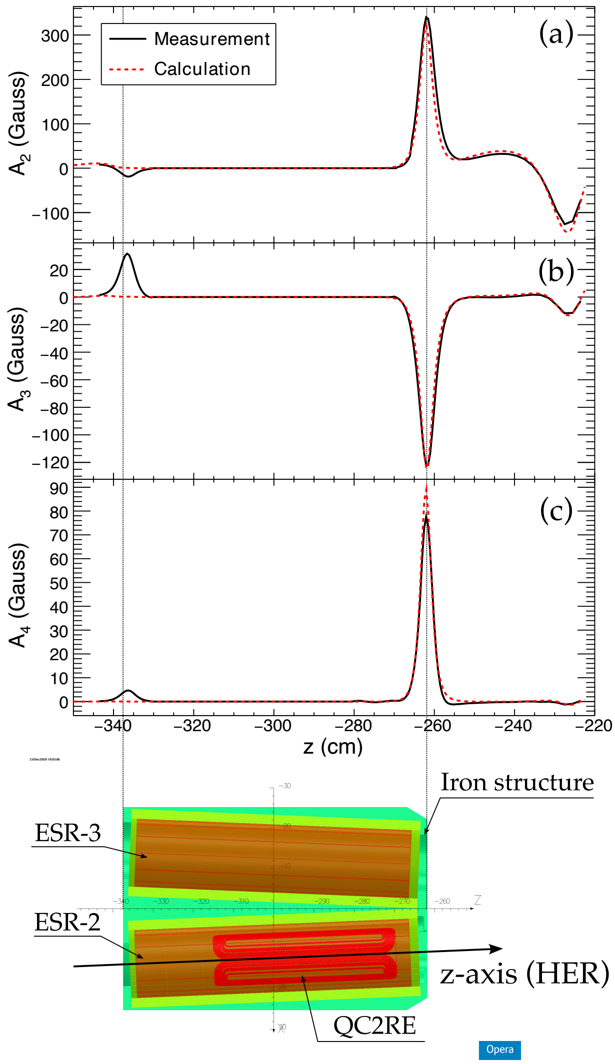

Figure 6: The axial profile of QC2RE. (a) The profile of skew quad, (b) the profile of skew sextupole, (c) the profile of skew octupole. The reference radius for these components is 35 mm. The horizontal axis is axial distance along HER axis and the origin is the IP. Solid lines are measurement result with the harmonic coil and the dashed curves are calculation results with Opera3D/TOSCA.

wire made of BeCu stretched from the end of the QCS cryostat through the beam pipe via the IP to the end of the other QCS cryostat. Both ends of the wire are fixed on precise x-y stages of the SSW units. The stretched wire's diameter and length are 0.1 mm and 9 m, respectively. We performed the SSW measurement with AC mode to separate the DC solenoid fields; we energized a quadrupole magnet with AC at 7.8125 Hz. Figure 7 shows the measured magnet center for the quadrupole field. The top two plots are x-direction offsets, and the bottom one is the vertical (y-) direction offsets of the magnet center. The left (right) plots are the HER (LER) magnet center. Black circles are the obtained offsets when the all-solenoid field is off, and the red squares are the offsets when the all-solenoids are on. Magnet positions varied with the solenoid fields turned on/off by dx ~ 0.1 mm, dy ~ 0.3 mm. The maximum horizontal (x-) offset is 0.7 mm for the QC1RP, and the maximum y-offset is −0.6 mm for the QC2LP. We can correct these quadrupole offsets with the dipole correctors and beam orbit tuning.

OPERATIONAL EXPERIENCE

Current Stability

The power supplies for QCS are IGBT type [8]. They supply stabilized current by the digital and analog feedback and achieved stability of 2 ppm a week. Figure 8 shows the one-week stability of the power supply for each main quadrupole magnet, and the red and blue lines are output current and correction voltage by digital feedback, respectively.

Failures

From 2018 to 2022, the QCS system experienced 62 power shutdown events by failures, such as magnet quench, the troubles of the power supplies, etc. Figure 9 shows the summary of failures from the start of SuperKEKB operation (Phase 3) to the long-shutdown 1. The gray, green, and blue bars are events caused by the troubles of the cooling water or the power supplies, the earthquake, and the beams, respectively.

The quench mechanism associated with the beam is not well understood, but from the fact that there was a sudden (about one μs)increase in coil voltage and background at Belle II detector, we deduce that the radiation originating from the beam deposited enough energy to cause the superconducting wire to quench.

At the early stage of the operation (2018), the magnet-quench related to the beam frequently happened, adjustment collimators or implementation of the fast abort system by Belle II detector significantly reduced the frequency of beam related quench event. The mechanism of the QCS failure by the earthquake is inferred as follows; when the earthquake happened, the relative distance varied between QCS solenoids and Belle II solenoid. And then, Faraday's induced voltage exceeds the threshold of the quench detector; as a result, the power supply moves to the shutdown process. The recovery time is typically one hour when the quadrupole magnet quenched, in the case of the compensation solenoids, ESL, or ESR1, it takes three to six hours.

Time Variation of Quadrupole Field

SuperKEKB is constant energy, so the quadrupole magnets in the QCS operate in dc mode. However, LER's vertical setting (model) tune varied after powering off/on the quadrupole magnet by 2×10^{-2} in a few hours.

Here, the model tune is a calculation tune from the lattice model with the operation current of the quadrupole magnets. The tune itself is kept constant by a tune feedback system. So, the drift of the model tune indicates some quadrupole magnetic field varies while the operation current is constant.

ISBN: 978-3-95450-236-3 ISSN: 2673-7027 doi:10.18429/JACoW-eeFACT2022-WEZAT0202

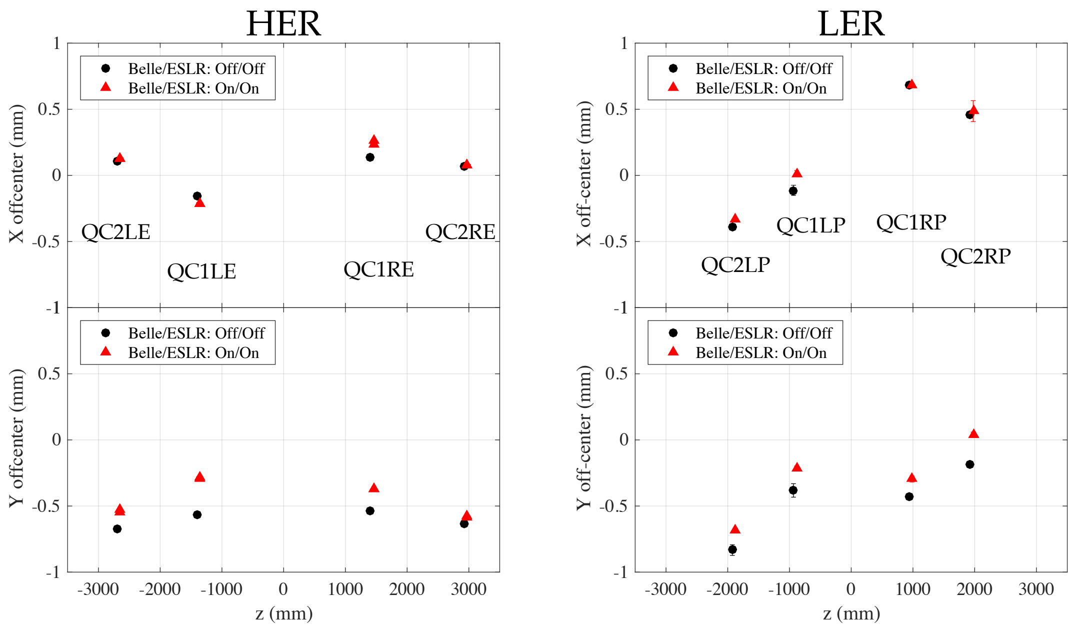

Figure 7: The offsets of magnet center from the target alignment position.

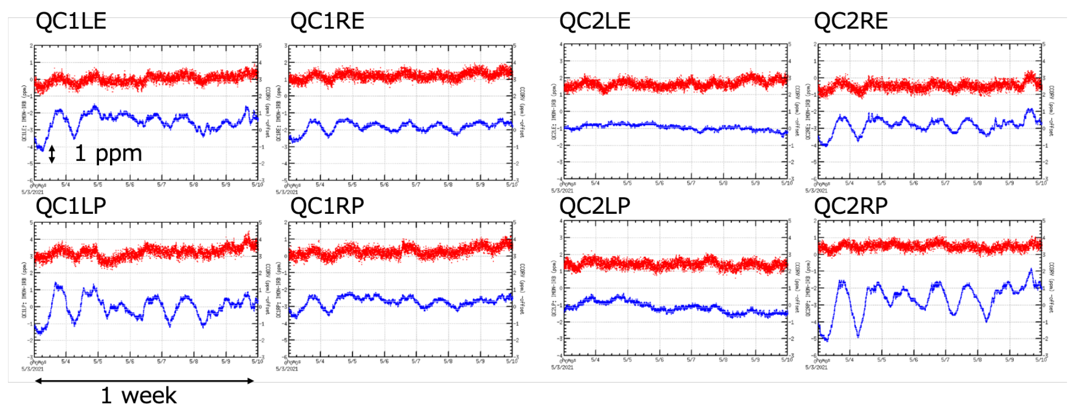

Figure 8: One week stability of power supply for each quadrupole magnets. The red and blue lines are output current and correction voltage by digital feedback, respectively.

Assuming the QCS quadrupole magnet caused this, the value of tune variation corresponds to the quadrupole field variation of ~2×10^{-4} on the QC1P.

Therefore, we performed measurements with the QC1P R&D magnet with the harmonic coil to confirm whether the magnetic field varies. Figure 10 shows the measured quadrupole components as a function of time. The black open and closed circles are obtained data by an energizing magnet current from 0 A to 1600 A. The red squares are the data by setting the current from 1638.3 A to 1600 A. The vertical axis is a ratio of the quadrupole variation, and is defined as follows;

$$\Delta R = \frac{C_2(t) - C_{20}}{C_{20}}. \quad (2)$$

Here, $C_2(t)$ is the amplitude of the quadrupole field at the time of t. The origin of the time is the setting time to the target magnet current. Furthermore, C_{20} is the quadrupole amplitude at $t \sim 2 \times 10^4$ at the down ramp. Figure 11 shows the recycling and ramping pattern. The plot exhibit that the quadrupole field varies by 3×10^{-4} in 7 hours as a function of $\log t$. This field variation is in the same order as the observed vertical-model tunes. We deduce that the flux creep in the superconductor cable cause this variation. Other accelerator facilities, such as Tevatron, DESY, and RHIC reported this phenomenon [9–11].

It depends on the ramping pattern of the magnet, and the optimized pattern suppresses the time variation. The obtained time variation energized after the optimized ramping is the red squares and is about 0.2×10^{-4}.

FUTURE UPGRADE OPTION

The SuperKEKB aims to achieve an integrated luminosity of 50 ab^{-1} around 2030. To achieve this, we need a luminosity of 6×10^{35} cm^{-2} s^{-1}. We have issues such as transverse-mode-coupling-instability, short-beam lifetime,

ISBN: 978-3-95450-236-3 ISSN: 2673-7027 doi:10.18429/JACoW-eeFACT2022-WEZAT0202

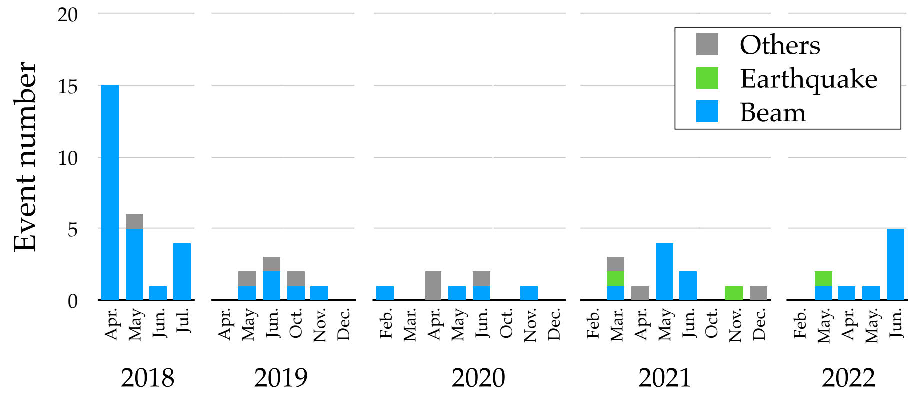

Figure 9: Summary of QCS failures.

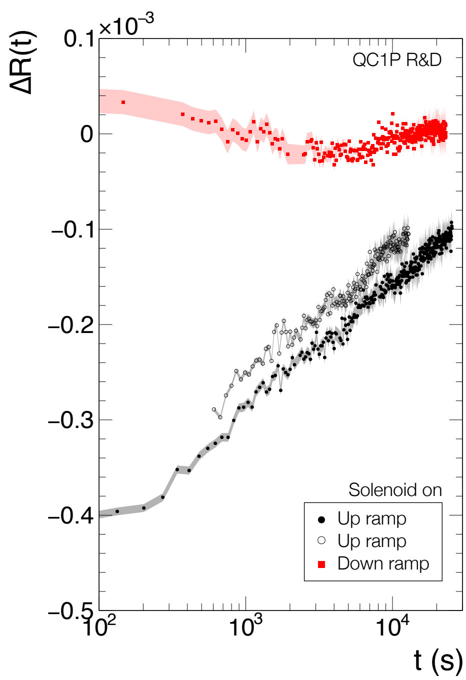

Figure 10: Time variation of quadrupole field of QC1P R&D magnet. The shaded areas are the uncertainties from the uncertainty of a thermal expansion of the harmonic-coil bobbin made of G10.

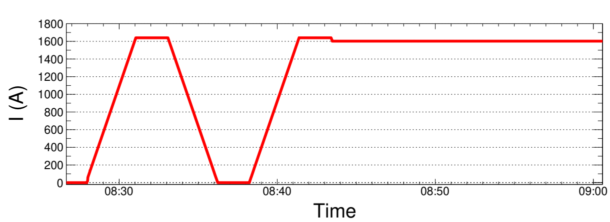

Figure 11: The optimized ramping pettern for QC1P magnet.

low-injection efficiency, and so on to increase the current luminosity. The QCS can contribute to improving beam lifetime. So we are investigating several upgrade options for the QCS. The upgrade is scheduled at long-shutdown-2 (LS2) period, which starts around 2027.

Although we are investigating the upgrade options, have yet to reach a final solution. The examples of the options which we have investigated so far are shown below;

- Moving the QC1P and QC1E away from the IP by 250 mm and 100 mm, respectively, and separating the compensation solenoid field and the main quadrupole field.
- Reducing the detector solenoid field from 1.5 T to 1.2 T.
- Increasing the inner radius of the corrector and setting the outer side of the main quadrupole magnet of QC1P.
- Getting QC1P and the compensation solenoid closer to IP by 300 mm.

After a detailed study, the options to move the magnets away from the IP and reduce the detector-solenoid field do not improve the luminosity.

Increasing the corrector's inner radius enables setting the corrector outside the main quadrupole magnet. As a result, we can enlarge the inner radius of the beam pipes at QC1P from 13.5 mm to 18.0 mm vertically and from 10.5 mm to 14.9 mm horizontally. Although this modification does not improve the beam lifetime, it is still open for discussion because it is expected that this reduces the beam background at the Belle II detector.

Moving the QC1P to the IP side by 300 mm is expected to increase the Touschek lifetime by ~ 2 times in calculation based on a simple lattice model. However, the option requires drastic modification at the IR, including the Belle II detector. Therefore, we need not only the design of the QCS but multifaceted investigation, such as how to install the detector and the QCS, impact on no BPM in the vicinity of the IP, further precise beam simulation, and the required time for the modification.

SUMMARY

On the upgrade from KEKB to SuperKEKB, we newly designed and constructed the QCS system for SuperKEKB. SuperKEKB requires the individual SC quadrupole magnets on the both ring, while KEKB had a common SC quadrupole magnet. As a result, the system is more complex than KEKB.

We performed the in-sites three kinds of magnetic measurements; the *B*-field multipole measurement, the magnet

ISBN: 978-3-95450-236-3 ISSN: 2673-7027 doi:10.18429/JACoW-eeFACT2022-WEZAT0202

center measurement, and the solenoid *B*-filed profile measurement. The field-multipole measurement results showed good qualities (less than 1-2 units) for all the quadrupole magnets except for the QC2RE magnet. When applying all the solenoid fields, the QC2RE magnet showed large multipole errors of 20 units for A_3 and 8 units for A_4. It is caused by the irregular shape at the iron structure end. The 3D magnetic analysis also represents this. The measured offsets of the magnet center were 0.7 mm at maximum, which is within range of a correction with the dipole correctors and the beam orbit tuning. The magnet center moved by 0.3 mm vertically by energizing the solenoid fields.

In the operation of SuperKEKB, the power supplies for the QCS are stable within 2 ppm a week. During the operation, we had many quenches associated with the beam. The typical recovery time was one hour and it is an acceptable time. We experienced shutdown by earthquake three times, because the induced voltage by earthquakes is sometimes over the threshold of the quench detector.

We are investigating upgrade options for the QCS to increase luminosity.

ACKNOWLEDGEMENTS

The authors are grateful to all the members of SuperKEKB accelerator and Belle II. The authors appreciate the engineers of Hitachi Technologies and Services. Finally, the authors express gratitude to the Mitsubishi Electric System & Service Co. engineers.

REFERENCES

[1] T. Abe *et al.*, “Achievements of KEKB,” *Prog. Theor. Exp. Phys.*, vol. 2013, no. 3, p. 03A001, 2013. doi:10.1093/ptep/pts102

[2] Y. Ohnishi *et al.*, “Accelerator design at SuperKEKB,” *Progr. Theor. Exp. Phys.*, vol. 2013, no. 3, p. 03A011, 2013. doi:10.1093/ptep/pts083

[3] Y. Onishi, “SuperKEKB luminosity quest,” in *Proc. eeFACT’22*, Frascati, Italy, Sep. 2022, paper MOXAT0103, this conference.

[4] K. Tsuchiya, N. Ohuchi, T. Ogitsu, T. Ozaki, and R. Sugahara, “Superconducting final focusing system for KEKB,” in in *PACS2001. Proc. 2001 Particle Accelerator Conf. (Cat. No.01CH37268)*, Chicago, IL, USA, Jun. 2001, pp. 3633-3635. doi:10.1109/PAC.2001.988202

[5] K. Tsuchiya, T. Ogitsu, N. Ohuchi, T. Ozaki, N. Toge, and H. Sakurabata, “Superconducting magnets for the interaction region of KEKB,” *IEEE Trans. Appl. Supercond.*, vol. 9, no. 2, pp. 1045–1048, 1999. doi:10.1109/77.783476

[6] N. Ohuchi *et al.*, “SuperKEKB beam final focus superconducting magnet system,” *Nucl. Instrum. Methods Phys. Res. Sect. A*, vol. 1021, p. 165930, 2022. doi:10.1016/j.nima.2021.165930

[7] Y. Arimoto *et al.*, “Magnetic measurement with single stretched wire method on SuperKEKB final focus quadrupoles,” in *Proc. IPAC’19*, Melbourne, Australia, May 2019, pp. 432-435. doi:10.18429/JACoW-IPAC2019-MOPMP006

[8] T. Oki, N. Tokuda, T. Adachi, N. Ohuchi, and S. Nakamura, “Full-scale prototype power supply for SuperKEKB final focus superconducting magnets,” *IEEE Trans. Appl. Supercond.*, vol. 26, no. 4, p. 0601404, 2016. doi:10.1109/TASC.2016.2523058

[9] R. Hanft, B. Brown, D. Herrup, M. Lamm, A. McInturff, and M. Syphers, “Studies of time dependence of fields in tevatron superconducting dipole magnets,” *IEEE Trans. Magn.*, vol. 25, no. 2, pp. 1647–1651, 1989. doi:10.1109/20.92616

[10] H. Brück *et al.*, “Time dependence of persistent current effects in the superconducting hera magnets,” in *11th Int. Conf. on Magnet Technology (MT-11)*, vol. 1, 1990, pp. 141–146. doi:10.1007/978-94-009-0769-0_24

[11] C. Liu, D. Bruno, A. Marusic, M. Minty, P. Thieberger, and X. Wang, “Mitigation of persistent current effects in the rhic superconducting magnets,” *Phys. Rev. Accel. Beams*, vol. 22, p. 111003, 2019. doi:10.1103/PhysRevAccelBeams.22.111003